

Assessing high-energy x-ray and proton irradiation effects on electrical properties of P-GaN and N-GaN thin films

Aoxue Zhong(钟傲雪), Lei Wang(王磊), Yun Tang(唐蕴), Yongtao Yang(杨永涛), Jinjin Wang(王进进), Huiping Zhu(朱慧平), Zhenping Wu(吴真平), Weihua Tang(唐为华), and Bo Li(李博)

Citation: Chin. Phys. B, 2023, 32 (**7**): 076102. DOI: 10.1088/1674-1056/accb8a

Journal homepage: http://cpb.iphy.ac.cn; http://iopscience.iop.org/cpb

What follows is a list of articles you may be interested in

Analysis of displacement damage effects on the charge-coupled device induced by neutrons at Back-n in the China Spallation Neutron Source

Yuan-Yuan Xue(薛院院), Zu-Jun Wang(王祖军), Wei Chen(陈伟), Xiao-Qiang Guo(郭晓强), Zhi-Bin Yao(姚志斌), Bao-Ping He(何宝平), Xu Nie(聂栩), Shankun Lai(赖善坤), Gang Huang(黄港), Jiang-Kun Sheng(盛江坤), Wu-Ying Ma(马武英), and Shi-Long Gou(缑石龙)

Chin. Phys. B, 2023, 32 (**7**): 076101. DOI: 10.1088/1674-1056/acac07

Atomic simulations of primary irradiation damage in U-Mo-Xe system

Wen-Hong Ouyang(欧阳文泓), Jian-Bo Liu(刘剑波), Wen-Sheng Lai(赖文生),Jia-Hao Li(李家好), and Bai-Xin Liu(柳百新)

Chin. Phys. B, 2023, 32 (**3**): 036101. DOI: 10.1088/1674-1056/ac9366

Microstructure and hardening effect of pure tungsten and ZrO_2 strengthened tungsten under carbon ion irradiation at 700℃

Chun-Yang Luo(罗春阳), Bo Cui(崔博), Liu-Jie Xu(徐流杰), Le Zong(宗乐), Chuan Xu(徐川), En-Gang Fu(付恩刚), Xiao-Song Zhou(周晓松), Xing-Gui Long(龙兴贵), Shu-Ming Peng(彭述明), Shi-Zhong Wei(魏世忠), and Hua-Hai Shen(申华海)

Chin. Phys. B, 2022, 31 (**9**): 096102. DOI: 10.1088/1674-1056/ac6b25

Angular dependence of proton-induced single event transient in silicon-germanium heterojunction bipolar transistors

Jianan Wei(魏佳男), Yang Li(李洋), Wenlong Liao(廖文龙), Fang Liu(刘方), Yonghong Li(李永宏), Jiancheng Liu(刘建成), Chaohui He(贺朝会), and Gang Guo(郭刚)

Chin. Phys. B, 2022, 31 (**8**): 086106. DOI: 10.1088/1674-1056/ac5d32

Introducing voids around the interlayer of AlN by high temperature annealing

Jianwei Ben(贲建伟), Jiangliu Luo(罗江流), Zhichen Lin(林之晨), Xiaojuan Sun(孙晓娟), Xinke Liu(刘新科), and Xiaohua Li(黎晓华)

Chin. Phys. B, 2022, 31 (**7**): 076104. DOI: 10.1088/1674-1056/ac3d7f

---

Assessing high-energy x-ray and proton irradiation effects on electrical properties of P-GaN and N-GaN thin films

Aoxue Zhong(钟傲雪)[1], Lei Wang(王磊)[2,†], Yun Tang(唐蕴)[2], Yongtao Yang(杨永涛)[1], Jinjin Wang(王进进)[3], Huiping Zhu(朱慧平)[2], Zhenping Wu(吴真平)[1], Weihua Tang(唐为华)[1,‡], and Bo Li(李博)[2]

[1] *State Key Laboratory of Information Photonics and Optical Communications & School of Science, Beijing University of Posts and Telecommunications, Beijing* 100876, *China*

[2] *Institute of Microelectronics and Key Laboratory of Science and Technology on Silicon Devices, Chinese Academy of Sciences; University of Chinese Academy of Sciences, Beijing* 100029, *China*

[3] *School of Integrated Circuits & State Key Laboratory of Information Photonics and Optical Communications, Beijing University of Posts and Telecommunications, Beijing* 100876, *China*

(Received 2 March 2023; revised manuscript received 5 April 2023; accepted manuscript online 10 April 2023)

The effects of ionizing and displacement irradiation of high-energy x-ray and 2-MeV proton on GaN thin films were investigated and compared in this study. The electrical properties of both P-GaN and N-GaN, separated from power devices, were gauged for fundamental analysis. It was found that the electrical properties of P-GaN were improved as a consequence of the disruption of the Mg–H bond induced by high-dose x-ray irradiation, as indicated by the Hall and circular transmission line model. Specifically, under a 100-Mrad(Si) x-ray dose, the specific contact resistance ρ_c of P-GaN decreased by 30%, and the hole carrier concentration increased significantly. Additionally, the atom displacement damage effect of a 2-MeV proton of 1×10^{13} p/cm^2 led to a significant degradation of the electrical properties of P-GaN, while those of N-GaN remained unchanged. P-GaN was found to be more sensitive to irradiation than N-GaN thin film. The effectiveness of x-ray irradiation in enhancing the electrical properties of P-GaN thin films was demonstrated in this study.

Keywords: x-ray radiation, proton radiation, GaN, circular transmission line model (CTLM)

PACS: 61.80.–x, 61.80.Cb, 73.61.–r, 73.61.Ey **DOI:** 10.1088/1674-1056/accb8a

1. Introduction

Wide bandgap semiconductors such as gallium nitride (GaN), silicon carbide (SiC), and gallium oxide (Ga_2O_3) have been extensively investigated in photoelectric and electronic devices owing to their exceptional material characteristics, including high photoelectric conversion efficiency, high breakdown electric field, high electron saturation drift velocity, and high mobility.[1–3] Notably, the advantageous tolerance of GaN-based devices to radiation damage has drawn special attention for their potential application in the aerospace sector.[4–6] Additionally, GaN-based devices are utilized in the aerospace industry due to their superior radiation damage resistance in a radiation environment.[7,8] In previous studies, most radiation effect research on GaN-based devices focused on performance degradation from the device's perspective.[9,10] The γ-ray irradiation effects on GaN Schottky diodes up to a γ-ray dose of 21 kGy were investigated.[11,12] Shammi Verma *et al.* analyzed the effect of various γ-ray irradiation doses on the parameters of Schottky diodes. The researchers discovered that the ideality factor initially increased and decreased at extremely high doses.[13] Proton damage on the steady-state and dynamic responses of PECVD-passivated GaN high electron mobility transistors (HEMTs) before and after 5-MeV proton irradiation was explained by a decrease in two-dimensional electron gas (2DEG) mobility and sheet carrier density.[14]

It is essential to characterize the irradiation damages of a power device and the damages of each component of the device to obtain a comprehensive understanding of irradiation damages. Several studies of irradiation effects on N-GaN have been reported previously.[15] However, a number of studies of irradiation effects on P-GaN films, which are the most crucial structural components in enhancement mode heterojunction high electron mobility transistors HEMTs and PIN diodes, is limited.[16] Low-energy protons irradiate enhancement mode GaN HEMTs with a P-GaN layer. Before using devices in radiation environments, it is also essential to consider the displacement and ionizing effects.[17,18] Previous research focused on a single study of electronic device displacement damage caused by proton irradiation. Experimental research comparing the effects of 380-keV proton irradiation on P-GaN and N-GaN based on two-terminal resistance dependence under the same conditions was published.[19] However, the effects of high doses of x-ray total ionizing dose irradiation on the P-type and N-type doping of GaN thin films have yet to be investigated. Radiation hardening engineering of GaN-based devices, such as InGaN/GaN multiple quanta well light emitting diodes, laser diodes, Schottky diodes, and AlGaN/GaN

†Corresponding author. E-mail: wangle@ime.ac.cn
‡Corresponding author. E-mail: whtang@bupt.edu.cn

© 2023 Chinese Physical Society and IOP Publishing Ltd

HEMTs requires evaluating the radiation damages of the atom displacement effect and the ionizing effect on GaN thin films and comparing the radiation tolerance between P-GaN and N-GaN epitaxial layers.[20]

Therefore, this work examined highdose x-ray ionizing effects on P-GaN and N-GaN thin films using Hall measurement and the circular transmission line model (CTLM). Additionally, the electrical property degradation of P-GaN and N-GaN under 2-MeV proton displacement effects was studied and compared in depth. Finally, behaviors of the ionizing effect and radiation damages of the displacement effect on P-type and N-type GaN thin films, including specific contact resistance, sheet resistance, carrier concentration, and mobility, were studied in detail.

2. Experimental details

As shown in Fig. 1(a) and Fig. 1(b), P-GaN and N-GaN structures were grown by metal–organic chemical vapor deposition (MOCVD) on a 2-inch (1 inch = 2.54 cm) *c*-plane sapphire substrate. First, a 5-μm buffer layer was grown on a substrate before 0.5-μm P-GaN (Mg: 1×10^{19} cm^{-3}) and 2-μm N-GaN (Si: 2×10^{19} cm^{-3}) were grown on the buffer layer. Then, after growth, Mg acceptors were activated through a 20-min thermal annealing process at 580 °C in N_2 ambient.

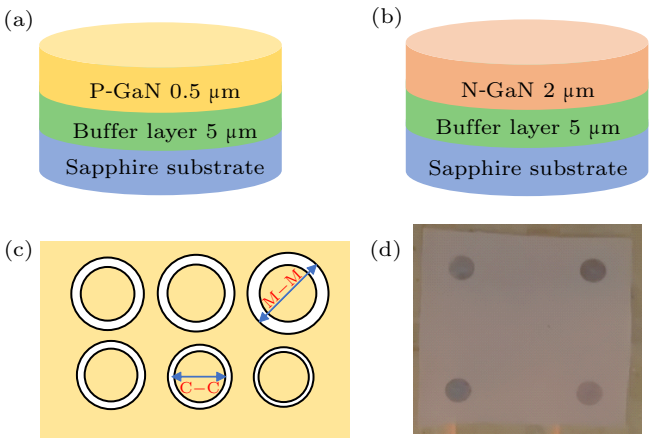


Fig. 1. Schematic cross section of (a) P-GaN and (b) N-GaN structures, (c) schematic plane section of CTLM measurement samples (C–C is the inside diameter and M–M is the outer diameter); (d) the photo of the Hall measurement samples.

Figures 1(c) and 1(d) display CTLM and Hall measurement samples. The CTLM method and Hall effect measurement were used to evaluate the electrical properties of GaN thin films exposed to radiation. For N-GaN Ohmic contact, a stack of Ti/Al/Ni/Au (with thicknesses respectively of 20/150/50/80 nm) was evaporated using e-beam evaporation before subjecting to rapid thermal annealing (RTA) at 850 °C for 30 s in N_2 ambience. Additionally, Ni/Au (10 nm/10 nm) was deposited on P-GaN followed by RTA at 550 °C for 420 s in an O_2 atmosphere, thereby forming Ohmic contact electrodes. The inner diameter of the CTLM pattern was 75 μm, while the outer diameters were 95 μm, 105 μm, 115 μm, 125 μm, 135 μm, and 145 μm, manufactured using a photolithographic lift-off process.

X-ray irradiation experiments were conducted at the Institute of High Energy Physics of the Chinese Academy of Sciences. The x-ray doses were set to 50 Mrad(Si), 100 Mrad(Si), and 150 Mrad(Si), with a dose rate of approximately 0.1 Mrad(Si), and the samples were exposed to room-temperature air. The proton irradiation experiments were conducted at the Institute of Technology and Peking University. The proton's energy and flux were 2 MeV and 1×10^{13} p/cm^2, respectively.

The *I*–*V* curves were measured using Keysight B4200A Precision Source/Measure Unit and Keysight B1505 Power Device Analyzer. In addition, HMS-5300 Hall equipment was used to measure carrier concentration and mobility.

3. Results and discussion

3.1. Electrical properties variations of P-GaN and N-GaN under high dose x-ray irradiation

Specific contact resistance ρ_c and sheet resistance R_{SH} were carried out through CTLM method.[21] The sheet resistance R_{SH} can be calculated via following formula:

$$R_{tot} = \frac{R_{sh}}{2\pi}\left[\ln\left(\frac{r_n}{r_0}\right) + L_T\left(\frac{1}{r_n}+\frac{1}{r_0}\right)\right], \tag{1}$$

where R_{tot} is the total resistance can be obtained via the fitting of *I*–*V* curve, r_0 and r_n is the radius of the inner and outer rings of CTLM structure, L_T is the transfer length.

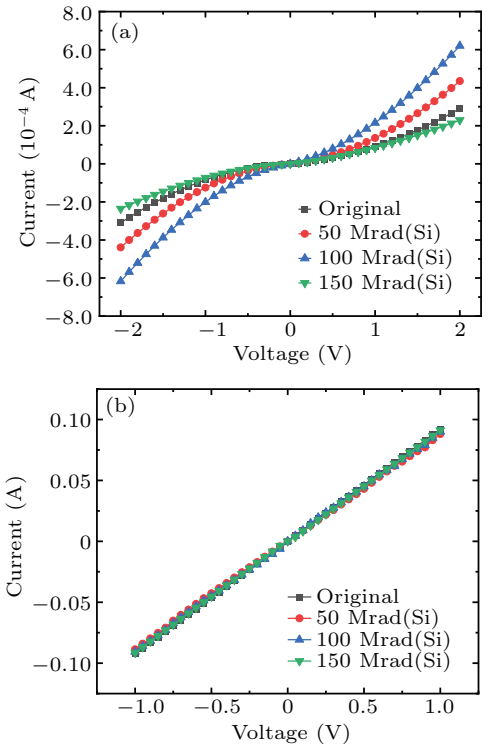


Fig. 2. The *I*–*V* curves of (a) P-GaN and (b) N-GaN CTLM samples under various x-ray radiation doses.

Figure 2(a) displays the *I*–*V* curves of P-GaN. The currents of irradiated P-GaN samples increased with increasing x-ray doses and then decreased at very high doses, whereas the current of irradiated N-GaN remained nearly unchanged. Table 1 displays the calculated ρ_c and R_{SH} values of the irradiated P-GaN and N-GaN samples at various x-ray doses. Under x-ray doses of 50 Mrad(Si) and 100 Mrad(Si), R_{SH} and ρ_c decreased significantly, indicating that both the P-GaN resistance and Ohmic contact were gradually enhanced. As depicted in Fig. 3, under x-ray doses of 50 Mrad(Si) and 100 Mrad(Si), the hole carrier concentration and mobility of P-GaN increased noticeably. Specifically, under 50 Mrad(Si) and 100 Mrad(Si), the hole concentration of P-GaN increased from 5.52×10^{17} cm^{-3} to 5.59×10^{17} cm^{-3} and 5.81×10^{17} cm^{-3}, respectively. Therefore, as the hole concentration in irradiated P-GaN increases, the electrical conductivity gradually improves. In addition, the width of the barrier region formed by metal/semiconductor contact decreases, improving P-GaN Ohmic contact.

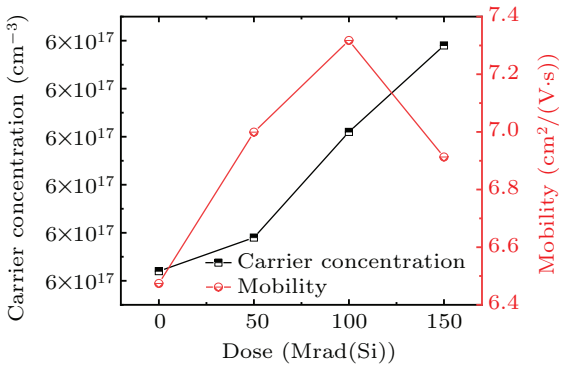


Fig. 3. Hole carrier concentration and hole carrier mobility of P-GaN samples under different x-ray doses.

It is well known that H elements are introduced from NH_3 decomposition and combine with Mg elements to form Mg–H complexes during the epitaxial growth of P-GaN.[22,23] The formed complexes, Mg–H, are charge-compensated and cannot be ionized to produce hole carriers, resulting in a low hole carrier concentration. In this instance, the increase in hole concentration with increasing x-ray doses could be attributed to x-ray radiation breaking the chemical bonds of Mg–H complexes through the interaction of the high-energy photon with the lattice.[24] Meanwhile, the holes' mobility of P-GaN increased from 6.47 cm^2·V^{-1}·s^{-1} to 6.98 cm^2·V^{-1}·s^{-1} under 50 Mrad(Si) and 7.33 cm^2·V^{-1}·s^{-1} under 100 Mrad(Si), indicating that the number of carrier scattering centers in P-GaN decreases after x-ray radiation.

It should be noted, however, that when the x-ray dose reaches 150 Mrad(Si) in this work, although ρ_c, R_{SH} and the carrier concentration of irradiated P-GaN increase, the carrier mobility decreases to some extent. As the x-ray dose increases, more Mg–H chemical bonds are broken, resulting in a high carrier concentration. It has been reported that GaN will generate nitrogen vacancies (V_N) in high ionizing radiation doses.[25,26] Along with the increase in x-ray dose, the ionization state variation of V_N generated in P-GaN could form double-site or even triple-site dopant-defect complexes.[27] The formed complexes act as scattering centers and ultimately reduce hole mobility, while the remaining Mg acceptors activated by x-rays increase carrier concentration. The formed Mg–V_N complexes cannot be ionized to generate hole carriers. Given that the hole carrier concentration of irradiated P-GaN is still rising, it is reasonable to assume that more Mg impurities are ionized, resulting in enhanced carrier scattering effects due to the ionized impurities. In this instance, the hole mobility decreased from 7.33 cm^2·V^{-1}·s^{-1} to 6.91 cm^2·V^{-1}·s^{-1}; however, the hole carrier concentration increased from 5.81 cm^{-3} to 5.99 cm^{-3}. Although the hole concentration continued to rise, the decrease in hole mobility for irradiated P-GaN has a significant impact on both ρ_c and R_{SH}. The ohmic contact of irradiated P-GaN began to degrade at a x-ray dose of 150 Mrad(Si). Therefore, using an appropriate dose of x-ray radiation can be an effective method to improve the conductivity of P-GaN.

Figure 2(b) illustrates the *I*–*V* curves of the irradiated N-GaN CTLM samples. Table 1 lists the electron carrier concentration and mobility of the irradiated N-GaN. The electrical parameters of N-GaN hardly degrade at various x-ray doses, indicating that N-GaN is more resistant to x-ray irradiation than P-GaN. This can be attributed to the fact that most Si dopants in N-GaN are already activated during epitaxial growth due to their lower activation energy. Therefore, since the lack of Si–H bonds in N-GaN, its conductivity could not be improved upon exposure to high-energy x-ray irradiation in the same manner as P-GaN.

Table 1. The measured and computational R_{SH}, ρ_c, carrier concentration and mobility of P-GaN and N-GaN samples under different x-ray irradiation dose.

	Dose (Mrad(Si))	Original	50	100	150
R_{SH} (Ω/□)	P-GaN	3.69×10^4	3.28×10^4	2.79×10^4	3.72×10^4
	N-GaN	0.161	0.163	0.164	0.167
ρ_c (Ω·cm^2)	P-GaN	0.11	0.073	0.031	0.147
	N-GaN	6.463×10^{-6}	6.464×10^{-6}	6.467×10^{-6}	6.468×10^{-6}
Carrier concentration (cm^{-3})	P-GaN	5.52×10^{17}	5.59×10^{17}	5.81×10^{17}	5.99×10^{17}
	N-GaN	1.18×10^{18}	1.10×10^{18}	1.12×10^{18}	1.15×10^{18}
Mobility (cm^2·V^{-1}·s^{-1})	P-GaN	6.474	6.999	7.317	6.913
	N-GaN	3.71×10^2	3.64×10^2	3.67×10^2	3.69×10^2

3.2. Comparison of irradiation damages between P-GaN and N-GaN by 2-MeV proton irradiation

In order to compare the degradation of electrical performance between P-GaN and N-GaN under displacement damage, GaN films were irradiated by 2-MeV proton with a fluence of 1×10^{13} p/cm^2.

Figure 4(a) shows *I*–*V* curves of original and irradiated P-GaN films, and the calculated ρ_c and R_{SH} are listed in Table 2. Under the fluence of 1×10^{13} p/cm^2, the R_{SH} increased from 3.69×10^4 Ω/□ to 4.16×10^4 Ω/□, while ρ_c increased from 0.11 Ω·cm^2 to 0.199 Ω·cm^2. The degradation of the ohmic contact quality was indicated by the increase in R_{SH} and ρ_c. Furthermore, the decrease in hole carrier concentration from 5.52×10^{17} cm^{-3} to 4.92×10^{17} cm^{-3} was attributed to the presence of radiation-induced defects such as V_N. These defects act as donor defects that can compensate for Mg acceptors in P-GaN. The formed Mg–V_N complex cannot generate holes, resulting in a decrease in the hole carrier concentration. Therefore, compared to the ionizing radiation effect, displacement damage caused a greater degradation in the quality of P-GaN films and the Ohmic contact.

Compared to the original N-GaN sample, the *I*–*V* curves of N-GaN showed little change and remained linear under the fluence of 1×10^{13} p/cm^2, as demonstrated in Fig. 4(b). It should be noted that slight changes were observed in the electron carrier concentration and mobility of irradiated N-GaN, as shown in Table 2. Although the impact of proton irradiation on N-type GaN films is minimal, the displacement damage resulting from proton radiation is more serious than the ionization effect caused by x-ray.

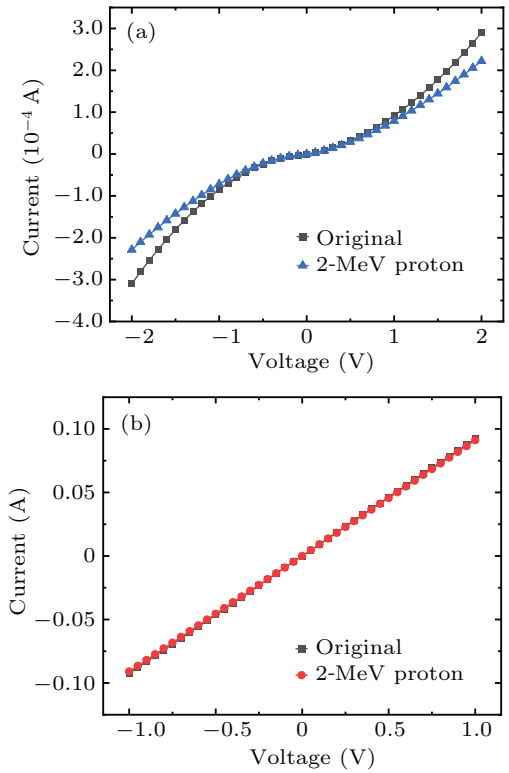


Fig. 4. The *I*–*V* curves of (a) P-GaN and (b) N-GaN CTLM samples under 2-MeV proton irradiation with fluence of 1×10^{13} p/cm^2.

Table 2. The measured R_{SH}, ρ_c, carrier concentration and mobility of P-GaN and N-GaN samples under 2-MeV proton irradiation.

Particles	R_{SH} (Ω/□)		ρ_c (Ω·cm^2)		Carrier concentration (cm^{-3})		Mobility (cm^2·V^{-1}·s^{-1})	
	P-GaN	N-GaN	P-GaN	N-GaN	P-GaN	N-GaN	P-GaN	N-GaN
Original	3.69×10^4	0.161	0.11	6.463×10^{-6}	5.52×10^{17}	1.18×10^{18}	2.79×10^4	3.71×10^2
2-MeV proton	4.16×10^4	0.165	0.199	6.478×10^{-6}	4.92×10^4	1.22×10^{18}	6.467×10^{-6}	3.59×10^2

In conclusion, the electrical properties of N-GaN were found to be almost unaffected by 2-MeV proton irradiation when compared to P-GaN, indicating that N-GaN has a better radiation tolerance (atom displacement effect) than P-GaN. Additionally, first-principles calculations suggest that the formation energy of native point defects, such as V_N, is much lower in P-GaN than in N-GaN, indicating that P-GaN generates more radiation-induced point defects than N-GaN at the same fluences.[28] This may explain the difference in radiation resistance between P-GaN and N-GaN thin films.

4. Conclusion

In this study, the effects of high energy x-ray and proton irradiation on GaN films were investigated by using Hall effect measurement and the CTLM method. The results revealed some novel phenomena. Firstly, the experimental data showed that x-ray irradiation could break the Mg–H chemical bond and increase the hole concentration and mobility in P-GaN. This finding demonstrates that x-ray irradiation can effectively enhance the electrical properties of P-GaN films. Secondly, x-ray irradiation had a more significant effect on P-GaN than N-GaN under the same radiation dose. Finally, the study showed that P-GaN is more sensitive to proton irradiation than N-GaN, suggesting that P-GaN films should be considered when assessing the total irradiation tolerance of GaN-based devices.

References

[1] Morya Ajay Kumar, Gardner Matthew C, Anvari Bahareh, Liu Liming, Yepes Alejandro G, Doval-Gandoy Jesus and Toliyat Hamid A 2019 *IEEE Trans. Transp. Electrif.* **5** 3

[2] Shi J, Zhang J, Yang L, Qu M, Qi D C and Zhang K H L 2021 *Adv. Mater.* **33** 50

[3] Zhang Q Y, Li N, Zhang T, Dong D M, Yang Y T, Wang Y H, Dong Z G, Shen J Y, Zhou T H, Liang Y L, Tang W H, Wu Z P, Zhang Y and Hao J H 2023 *Nat. Commun.* **14** 418

[4] Keshmiri N, Wang D, Agrawal B, Hou R and Emadi A 2020 *IEEE Access* **8** 70553
[5] Jiang X, Li C H, Yang S X, Liang J H, Lai L K, Dong Q Y, Huang W, Liu X Y and Luo W J 2023 *Chin. Phys. B* **32** 037201
[6] Zhang Y, Dadgar A and Palacios T 2018 *J. Phys. D* **51** 273001
[7] Javier B F, Jesús M C A, José F S O and Erika L P 2021 *Electronics* **10** 677
[8] Lin Z Z, Lü L, Zheng X F, Cao Y R, Hu P P, Fang X and Ma X H 2022 *Chin. Phys. B* **31** 036103
[9] Wu Y, Zhang J, Zhao S, Wu Z, Wang Z, Mei B, Duan C, Zhao D, Zhang W, Liu Z and Hao Y 2022 *Sci. China Inf. Sci.* **65** 182404
[10] Liu Y a and Luo W 2018 *J. Semicond.* **39** 074005
[11] Umana-Membreno G A, Dell J M, Hessler T P, Nener B D, Parish G, Faraone L and Mishra U K 2002 *Appl. Phys. Lett.* **80** 4354
[12] Umana-Membreno G A, Dell J M, Parish G, Nener B D, Faraone L and Mishra U K 2003 *IEEE Trans. Electron Dev.* **50** 2326
[13] Shammi Verma K C P, Achamma Bobby, and Dinakar Kanjilal 2014 *IEEE Trans. Dev. Mate. Reliability* **14** 721
[14] Xi Y, Hsieh Y L, Hwang Y H, Li S, Ren F, Pearton S J, Patrick E, Law M E, Yang G, Kim H Y, Kim J, Baca A G, Allerman A A and Sanchez C A 2014 *J. Vac. Sci. Technol. B* **32** 012201
[15] Kumar S, Mariswamy V K, Kumar A, Kandasami A and Sannathammegowda K 2020 *ECS J. Solid State Sci.* **9** 093017
[16] Fan J B, Ling S Y, Liu H X, Duan L, Zhang Y, Guo T T, Wei X and He Q 2020 *Chin. Phys. B* **29** 117701
[17] Wan X, Baker O K, McCurdy M W, Zhang E X, Zafrani M, Wainwright S P, Xu J, Bo H L, Reed R A, Fleetwood D M and Ma T P 2017 *IEEE Trans. Nucl. Sci.* **64** 253
[18] Yang Y T, Zhu H P, Wang L, Jiang Y C, Wang T Q, Liu C M, Li B, Tang W H, Wu Z P, Yang Z B and Li D F 2022 *Mater. & Des.* **221** 110944
[19] Okada H, Okada Y, Sekiguchi H, Wakahara A, Sato S i and Ohshima T 2014 *IEICE Trans. Electron* E97.C 409
[20] Kaplar R J, Allerman A A, Armstrong A M, Crawford M H, Dickerson J R, Fischer A J, Baca A G and Douglas E A 2017 *ECS J. Solid State Sci. Technol.* **6** Q3061
[21] Li X J, Zhao D G, Jiang D S, Chen P, Zhu J J, Liu Z S, Le L C, Yang J, He X G, Zhang L Q, Liu J P, Zhang S M and Yang H 2015 *Chin. Phys. B* **24** 096804
[22] Tetsuo N, Nobuyuki I, Kazuyoshi T, Kataoka K and Kachi T 2018 *J. Appl Phys.* **124** 165706
[23] Li W, Nomoto K, Lee K, Islam S M, Hu Z, Zhu M, Gao X, Xie J, Pilla M, Jena D and Xing H G 2018 *Appl. Phys. Lett.* **113** 062105
[24] Xingze H, Xinwen Z and Kuo C C J 2013 *IEEE Access* **1** 67
[25] Polyakov A Y, Pearton S J, Frenzer P, Ren F, Liu L and Kim J 2013 *J. Mater. Chem. C* **1** 877
[26] Pearton S J, Deist R, Ren F, Liu L, Polyakov A Y and Kim J 2013 *J. Vac. Sci. Technol. A* **31** 050801
[27] Huang M, Li H and Chen S 2021 *Phys. Status Solidi A* **218** 2000723
[28] Van de Walle C G and Neugebauer J 2004 *J. Appl. Phys.* **95** 3851